



Precise and highly-sensitive Doppler-free two-photon absorption dual-comb spectroscopy using pulse shaping and coherent averaging for fluorescence signal detection

AKIKO NISHIYAMA,^{1,2,3} YOSHIKI NAKAJIMA,^{1,2} KEN'ICHI NAKAGAWA,¹ AND KAORU MINOSHIMA^{1,2,*}

¹Department of Engineering Science, Graduate School of Informatics, University of Electro-Communications (UEC), 1-5-1 Chofugaoka, Chofu, Tokyo 182-8585, Japan

²Japan Science and Technology Agency (JST), ERATO MINOSHIMA Intelligent Optical Synthesizer (IOS) Project, 1-5-1 Chofugaoka, Chofu, Tokyo 182-8585, Japan

³Research Fellow of the Japan Society for the Promotion of Science (JSPS), 1-5-1 Chofugaoka, Chofu, Tokyo 182-8585, Japan

*k.minoshima@uec.ac.jp

Abstract: We demonstrated Doppler-free two-photon absorption dual-comb spectroscopy of $5S_{1/2} - 5D_{3/2}$ and $5D_{5/2}$ transitions of Rb. We employed simple pulse-shaping of the dual-comb source and eliminated Doppler-broadening backgrounds, which cause fitting errors of the Doppler-free signals. Moreover, to improve sensitivity, we investigated the coherence in dual-comb fluorescence signals and the coherent averaging method was applied to fluorescence dual-comb detection for the first time. The detection sensitivity was significantly improved by coherent averaging to reduce the noise floor. Observed Doppler-free spectra was fitted to Voigt profiles and we performed absolute frequency determination with a precision of about 100 kHz.

© 2018 Optical Society of America under the terms of the [OSA Open Access Publishing Agreement](#)

OCIS codes: (300.6320) Spectroscopy, high-resolution; (140.4050) Mode-locked lasers; (300.6210) Spectroscopy, atomic.

References and links

1. E. Baumann, F. R. Giorgetta, W. C. Swann, A. M. Zolot, I. Coddington, and N. R. Newbury, "Spectroscopy of the methane ν_3 band with an accurate midinfrared coherent dual-comb spectrometer," *Phys. Rev. A* **84**(6), 062513 (2011).
2. A. M. Zolot, F. R. Giorgetta, E. Baumann, W. C. Swann, I. Coddington, and N. R. Newbury, "Broad-band frequency references in the near-infrared: Accurate dual comb spectroscopy of methane and acetylene," *Quant. Spectrosc. Radiat. Transf.* **118**, 26–39 (2013).
3. S. Okubo, K. Iwakuni, K. M. T. Yamada, H. Inaba, A. Onae, F.-L. Hong, and H. Sasada, "Transition dipole-moment of the $\nu_1 + \nu_3$ band of acetylene measured with dual-comb Fourier-transform spectroscopy," *J. Mol. Spectrosc.* **341**, 10–16 (2017).
4. I. Coddington, N. Newbury, and W. Swann, "Dual-comb spectroscopy," *Optica* **3**(4), 414–426 (2016).
5. P. Jacquet, J. Mandon, B. Bernhardt, R. Holzwarth, G. Guelachvili, T. W. Hänsch, and N. Picqué, "Frequency Comb Fourier Transform Spectroscopy with kHz Optical Resolution," in *Fourier Transform Spectroscopy*, OSA Technical Digest (CD) (Optical Society of America, 2009), paper FMB2.
6. S. Okubo, Y.-D. Hsieh, H. Inaba, A. Onae, M. Hashimoto, and T. Yasui, "Near-infrared broadband dual-frequency-comb spectroscopy with a resolution beyond the Fourier limit determined by the observation time window," *Opt. Express* **23**(26), 33184–33193 (2015).
7. A. Nishiyama, S. Yoshida, Y. Nakajima, H. Sasada, K. Nakagawa, A. Onae, and K. Minoshima, "Doppler-free dual-comb spectroscopy of Rb using optical-optical double resonance technique," *Opt. Express* **24**(22), 25894–25904 (2016).
8. T. Ideguchi, B. Bernhardt, G. Guelachvili, T. W. Hänsch, and N. Picqué, "Raman-induced Kerr-effect dual-comb spectroscopy," *Opt. Lett.* **37**(21), 4498–4500 (2012).
9. T. Ideguchi, S. Holzner, B. Bernhardt, G. Guelachvili, N. Picqué, and T. W. Hänsch, "Coherent Raman spectro-imaging with laser frequency combs," *Nature* **502**(7471), 355–358 (2013).
10. B. Lomsadze and S. T. Cundiff, "Frequency comb-based four-wave-mixing spectroscopy," *Opt. Lett.* **42**(12), 2346–2349 (2017).
11. A. Hipke, S. A. Meek, T. Ideguchi, T. W. Hänsch, and N. Picqué, "Broadband Doppler-limited two-photon and stepwise excitation spectroscopy with laser frequency combs," *Phys. Rev. A* **90**(1), 011805 (2014).

12. A. Hipke, S. A. Meek, G. Guelachvili, T. W. Hänsch, and N. Picqué, "Doppler-free broad spectral bandwidth two-photon spectroscopy with two laser frequency combs," in Conference on Lasers and Electro Optics (Optical Society of America, 2013), paper CTh5C.8.
13. S. A. Meek, A. Hipke, G. Guelachvili, T. W. Hänsch, and N. Picqué, "Doppler-free Fourier transform spectroscopy," *Opt. Lett.* **43**(1), 162–165 (2018).
14. A. Hipke, (2016) "Dual-frequency-comb two-photon spectroscopy," Dissertation, LMU München: Faculty of Physics, <https://edoc.ub.uni-muenchen.de/19360/>.
15. R. Teets, J. Eckstein, and T. W. Hänsch, "Coherent two-photon excitation by multiple light pulses," *Phys. Rev. Lett.* **38**(14), 760–764 (1977).
16. J. N. Eckstein, A. I. Ferguson, and T. W. Hänsch, "High-resolution two-photon spectroscopy with picosecond light pulses," *Phys. Rev. Lett.* **40**(13), 847–850 (1978).
17. P. Fendel, S. D. Bergeson, T. Udem, and T. W. Hänsch, "Two-photon frequency comb spectroscopy of the 6s-8s transition in cesium," *Opt. Lett.* **32**(6), 701–703 (2007).
18. S. Y. Zhang, J. T. Wu, Y. L. Zhang, J. X. Leng, W. P. Yang, Z. G. Zhang, and J. Y. Zhao, "Direct frequency comb optical frequency standard based on two-photon transitions of thermal atoms," *Sci. Rep.* **5**(1), 15114 (2015).
19. A. Nishiyama, K. Nakashima, A. Matsuba, and M. Misono, "Doppler-free two-photon absorption spectroscopy of rovibronic transition of naphthalene calibrated with an optical frequency comb," *J. Mol. Spectrosc.* **318**, 40–45 (2015).
20. M. Misono, J. Wang, M. Ushino, M. Okubo, H. Katô, M. Baba, and S. Nagakura, "Doppler-free two-photon absorption spectroscopy and the Zeeman effect of the $A^1B_{2u} \leftarrow X^1A_{1g} 14_0^1 1_0^1$ band of benzene," *J. Chem. Phys.* **16**(1), 162–272 (2002).
21. I. Barmes, S. Witte, and K. S. E. Eikema, "High-Precision Spectroscopy with Counterpropagating Femtosecond Pulses," *Phys. Rev. Lett.* **111**(2), 023007 (2013).
22. J. Wu, D. Hou, Z. Qin, X. Dai, Z. Zhang, and J. Zhao, "Erbium fiber laser-based direct frequency comb spectroscopy of Rb two-photon transitions," *Opt. Lett.* **38**(23), 5028–5031 (2013).
23. I. Coddington, W. C. Swann, and N. R. Newbury, "Coherent linear optical sampling at 15 bits of resolution," *Opt. Lett.* **34**(14), 2153–2155 (2009).
24. I. Coddington, W. C. Swann, and N. R. Newbury, "Coherent dual-comb spectroscopy at high signal-to-noise ratio," *Phys. Rev. A* **82**(4), 043817 (2010).
25. J. Snadden, R. Clarke, and E. Riis, "FM spectroscopy in fluorescence in laser-cooled rubidium," *Opt. Commun.* **152**(4–6), 283–288 (1998).
26. Y. Nakajima, H. Inaba, K. Hosaka, K. Minoshima, A. Onae, M. Yasuda, T. Kohno, S. Kawato, T. Kobayashi, T. Katsuyama, and F.-L. Hong, "A multi-branch, fiber-based frequency comb with millihertz-level relative linewidths using an intra-cavity electro-optic modulator," *Opt. Express* **18**(2), 1667–1676 (2010).
27. D. Sheng, A. Pérez Galván, and L. A. Orozco, "Lifetime measurements of the 5d states of rubidium," *Phys. Rev. A* **78**(6), 062506 (2008).
28. T. J. Quinn, "Practical realization of the definition of the metre, including recommended radiations of other optical frequency standards (2001)," *Metrologia* **40**(2), 103–133 (2003).

1. Introduction

Dual-comb spectroscopy opens up new possibilities of molecular and atomic spectroscopy as attractive precise spectroscopic tools [1–3]. Dual-comb spectroscopy enables us to simultaneously measure a broadband spectrum with the high resolution of the comb mode intervals and high frequency precision of the stabilized comb modes [4]. Furthermore, it is possible to obtain higher resolution than the mode intervals thanks to the narrow comb mode linewidths [5,6]. We have already demonstrated precise atomic spectroscopy with sub-Doppler resolution using the dual-comb and optical-optical double-resonance spectroscopic scheme [7].

Most of the dual-comb studies that are based on absorption spectroscopy detect the linear absorptions, but since the frequency combs have properties as ultrashort pulses, the dual-combs can also be applied to nonlinear spectroscopic techniques, such as stimulated Raman scattering [8], coherent anti-Stokes Raman scattering [9], and four wave mixing [10] spectroscopies. Furthermore, pioneering studies of the dual-comb application to two-photon absorption spectroscopy have been reported by Picqué et al. [11–14]. In the direct comb excitation of two-photon transitions, many comb mode pairs with the same sum frequencies contribute to a transition, and non-resonant two-photon transitions that are nonlinear processes are observable [15–17]. Single-comb two-photon absorption spectroscopy was also reported, and that is of great interest to the direct stabilization of comb mode to an atomic reference [18]. However, it is difficult to assign unknown lines using the single-comb spectroscopy because we have no means of knowing the mode numbers contributing to the two-photon transitions. On the other hand, the dual-comb two-photon absorption spectroscopy is based on Fourier transform spectroscopy; thus,

broadband two-photon absorption spectra are attainable simultaneously. Moreover, the two-photon excitation with counter-propagating photons causes a Doppler-free spectrum [12–14]. Doppler-free two-photon absorption spectroscopy is an important technique in the field of high-resolution molecular spectroscopy for the study of dynamics in electronic excited states, due to the observations with different selection rules from one-photon transitions [19,20].

In this study, we performed Doppler-free two-photon absorption dual-comb spectroscopy. The basic configuration of the spectroscopic system is based on the previous studies of Refs. 11–14. And to achieve greater precision of the frequency measurement of spectra, we used simple pulse shaping of frequency combs and eliminated the Doppler-broadening background. The background reduction technique was proposed in previous studies of single-comb two-photon spectroscopy [21,22], and we applied the technique to dual-comb spectroscopy for the first time. In addition, we demonstrated sensitivity improvement by applying coherent averaging [23,24] of fluorescence signals. Coherent averaging is a basic technique for dual-comb spectroscopy. However, the technique has been not applied before to background-free detections, such as fluorescence signal [11–14] or anti-Stokes signal [9] detections, to the best of our knowledge. In this paper, we show the remarkable effect of coherent averaging on the noise floor reduction in fluorescence dual-comb signals. We measured fully-resolved hyperfine spectra of $5S_{1/2} - 5D_{5/2}$ and $5D_{3/2}$ transitions of ^{87}Rb and ^{85}Rb simultaneously, and determined absolute frequencies of the spectra with a precision of about 100 kHz.

2. Principle and experiment

2.1 Principle of Doppler-free two-photon absorption spectroscopy using dual-comb

The principle of two-photon absorption spectroscopy using a dual-comb is illustrated in Fig. 1(a) [11]. As is well known in the studies of single-comb two-photon spectroscopy, mode pairs of a comb with a same sum frequency as the two-photon resonance introduce the transition. There is an excessively large number of possible pairs, $f_n + f_m, f_{n-1} + f_{m+1}, f_{n-2} + f_{m+2}, \dots$, more than ten thousand in our experiment, where f_n and f_m are comb mode frequencies with the mode numbers of n and m , respectively. The contribution of many modes enables us to observe the non-resonant two-photon transitions in spite of the low power of each comb mode, which are sub-microwatt. In dual-comb two-photon absorption spectroscopy, two combs excite the same transition with the difference of excitation frequency of $(m+n)\Delta f_{\text{rep}} + 2\Delta f_{\text{ceo}}$, where Δf_{rep} and Δf_{ceo} are the difference of the repetition frequencies and offset frequencies of the two combs, respectively. For simplicity, we assume that a transition is introduced by each comb mode pair with the same sum mode numbers, $m+n$. The difference of excitation frequencies creates a modulation of the excited state population [25]. The fluorescence intensity is proportional to the modulated population in the excited state, so that we observe the beat with the frequency of $(m+n)\Delta f_{\text{rep}} + 2\Delta f_{\text{ceo}}$ in the fluorescence signal. The beat frequency in the fluorescence gives a value of $m+n$ because the other values are already known. Therefore, dual-comb two-photon spectroscopy based on fluorescence detection reveals the two-photon absorption spectra not the fluorescence spectra. In our study, a dual-comb source excites the $5S_{1/2} - 5D_{5/2}$ and $5D_{3/2}$ transitions of Rb at the 778 nm two-photon transition, and subsequent decay via the $6P_{3/2}$ and $6P_{1/2}$ states yields the fluorescence at 420 nm. A small portion of the comb spectra also introduces resonant stepwise transition, $5S_{1/2} - 5P_{3/2} - 5D_{5/2, 3/2}$ states, which provide an enhancement of transition intensities.

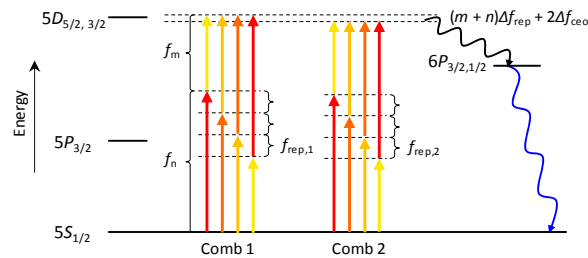


Fig. 1. Energy level diagram for two-photon transition in $^{85,87}\text{Rb}$. Non-resonant $5S - 5D$ transitions ($2 \times 778 \text{ nm}$) and stepwise $5S - 5P - 5D$ (780nm , 776 nm) transitions are excited by using the pair of comb modes. Excited atoms decay from $5D$ states to ground states via the $6P$ state with a fluorescence at 420 nm .

In two-photon absorption spectroscopy, two counter-propagating photons reduce the Doppler-broadenings [12–14]. The Doppler-free signals can be obtained at the small region where the counter-propagating pulses overlap, and Doppler-broadened transitions that are introduced by two co-propagating photons occur anywhere on the beam path. The Doppler-broadened spectra also appear in Doppler-free measurements as a Doppler-broadening background.

2.2 Experimental setup

Figure 2 shows the experimental setup for Doppler-free two-photon absorption dual-comb spectroscopy. Our dual-comb source is two home-made Er: fiber-based mode-locked lasers operating in the $1.55 \mu\text{m}$ spectral region with slightly different repetition frequencies of about 56.6 MHz . The two combs are phase-locked using the same scheme as [7]. The repetition frequency ($f_{\text{rep},1}$) of comb1 and offset frequencies ($f_{\text{CEO},1}$ and $f_{\text{CEO},2}$) are phase-locked to radio frequency (RF) signals referencing a global-positioning-system (GPS)-disciplined clock with an uncertainty of 3×10^{-12} in 1 s to precisely determine absolute transition frequencies. A mode of comb2 is phase locked to a continuous wave (CW) laser that is locked to a mode of comb1. An electro-optical modulator included in the laser cavity of comb2 enables high-speed control of the effective cavity length [26] and achieves a sufficiently narrow relative linewidth and long coherence time between the two combs.

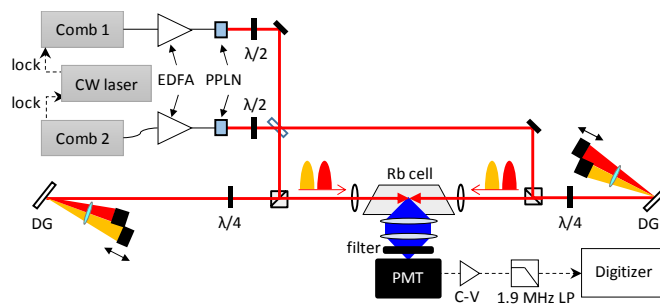


Fig. 2. Experimental setup for Doppler-free two-photon absorption spectroscopy. EDFA: Er-doped fiber amplifiers, PPLN: periodically-poled lithium niobate, DG: diffraction grating, PMT: photomultiplier tube, C-V: current-to-voltage converter, LP: low-pass filter.

The outputs of the two combs are amplified to 120 mW by Er-doped fiber amplifiers (EDFAs), and periodically-poled lithium niobates (PPLNs) are used for second-harmonic generation (SHG). The PPLNs have periods of $19.4 \mu\text{m}$ and lengths of 5 mm , and these are heated to $70 \text{ }^\circ\text{C}$. The SHG have a center wavelength of 778 nm , full-width half-maximum (FWHM) of 5 nm , and maximum power of 40 mW . After the PPLN, the two beams are overlapped and split to the two arms. To eliminate the Doppler-broadening background, we employ the split-pulse technique [21,22]. In each arm, the beams are

dispersed by a diffraction grating (DF) and the two color parts of the comb spectra, one longer and one shorter than the transition wavelength (778 nm), are reflected back by two mirrors with an adjustable delay that changes the time delay of the split sub pulses. The split co-propagating pulses cannot cause the two-photon transitions because components of the mode pairs are separated into each sub pulse, which have no temporal overlap. The counter-propagating reflected pulses from the two arms are linearly polarized and focused on the center of a cell using 75 mm focal length lenses. The cell is filled with ^{85}Rb and ^{87}Rb isotopes, which are mixed according to their natural abundances. And the cell is covered with magnetic shielding box in order to reduce the Zeeman shifts caused by external magnetic fields. The path lengths of the two arms are adjusted to be equal so that the refracted pulses from the two paths overlap at the center of the cell. The fluorescence signal is collimated onto a photomultiplier tube (PMT, Hamamatsu, H1924), and we used a color filter to reduce the scattered light source. Observed fluorescence signals are amplified by a current-to-voltage converter (C6438-01), and low-pass filtered signals are digitized by a 14-bit digitizer (NI PX1e-5122).

2.3 Detail of the measurement conditions

The modulation frequency of the excited-state population is limited by lifetimes of the excited states [11,25]. The lifetime of the $5D_{5/2}$ state of Rb is about 240 ns, and corresponding natural width is 660 kHz [27]. The fluorescence rate follows the excitation rate modulation when the modulation is sufficiently slow compared with the upper-state lifetime. In our experiments, parameters of two comb frequencies are set to be able to obtain the fluorescence beat at roughly the same or lower frequency than the natural width of the transition to avoid the limitation. For example, we choose the frequencies $f_{\text{rep},1} = 56.604\ 100\ \text{MHz}$, $f_{\text{rep},2} = 56.604\ 000\ \text{MHz}$, and $\Delta f_{\text{ceo}} = f_{\text{ceo},1} - f_{\text{ceo},2} = -1.09\ \text{MHz}$. In this case, fluorescence beat frequencies of the $5S_{1/2} - 5D_{5/2}$ transition at 770.57 THz appear at 660 kHz. The sum mode number $m + n$ for comb1 is approximately 13613350, thus the beat frequency is $(m + n)\Delta f_{\text{rep}} + 2\Delta f_{\text{ceo}} = 660\ \text{kHz} + 24f_{\text{rep},2}$. The last term can be ignored because it indicates a difference of sum mode numbers between two combs.

3. Experimental results

3.1 Observed Doppler-limited and Doppler-free spectra

Figure 3(a) shows a time domain fluorescence signal obtained by co-propagating pulses. One of the arms of optical paths in Fig. 2 was blocked and the delay in the other path was removed. The total incident power was 40 mW, averaging time of this measurement was 20 s, and the temperature of the Rb cell was 100 °C in both of the measurements in Fig. 3. A Fourier transform of the fluorescence signal yields the Doppler-limited two-photon absorption spectra of $5S_{1/2} - 5D_{5/2}$ and $5D_{3/2}$ transitions simultaneously as shown in Fig. 3(b). The spectral linewidths are several GHz due to Doppler-broadenings and overlaps of hyperfine transitions.

Figures 3(c) and (d) respectively show the time-domain fluorescence signal and spectrum obtained by Doppler-free measurement using the setup described in Fig. 2. The split pulse delays were set to 10 mm, and the incident power from each direction was 10 mW. To realize higher-resolution than the comb mode intervals, the mode frequencies of the combs are scanned by varying $f_{\text{rep},1}$. The scan step of mode frequencies are 400 kHz corresponding 0.03 Hz scan step of $f_{\text{rep},1}$, and averaging time was 40 s for each $f_{\text{rep},1}$ value. The observed spectrum shows sharp Doppler-free lines of the $5S_{1/2} - 5D_{5/2}$ and $5D_{3/2}$ transitions. We can see the hyperfine splitting of the $5S_{1/2}$ states of two isotopes in Fig. 3(d). The hyperfine splittings of the upper levels can also be resolved in further magnified views, which are shown in section 3.4.

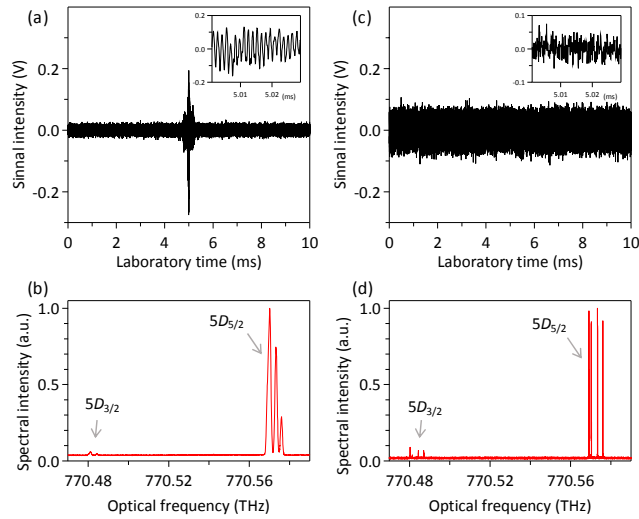


Fig. 3. (a) Time-domain fluorescence signal measured by co-propagating pulses. The inset shows a magnified view of around center burst signal. (b) Doppler-limited two-photon absorption spectrum (770.47 – 770.59 THz) including the $5S_{1/2} - 5D_{5/2}$ and $5D_{3/2}$ transitions obtained from FFT of (a) averaged over 20 s. (c) Fluorescence signal measured by counter-propagating pulses. The inset shows a magnified view of a part of the signal. (d) Doppler-free spectrum showing same region of (b). The spectrum was obtained from FFTs of fluorescence signals averaged over 40 s, and frequency intervals are interleaved by frequency scan of the comb modes.

3.2 Reduction of Doppler-broadening background

We demonstrate the effect of pulse splitting for the reduction of Doppler-broadening background in dual-comb spectroscopy. Figure 4 shows three spectra of the $5S_{1/2} - 5D_{5/2}$ transition obtained by the Doppler-free measurement with different delays of the split pulses. Incident powers are 10 mW, and cell temperature was 100 °C. In Fig. 4, green, blue, and red lines represent the spectra observed by pulses with the delays of 1 mm, 5 mm, and 10 mm, respectively. The delays of pulses in the two arms are adjusted to be equal. In one arm, longer wavelength parts are delayed from the shorter wavelength parts, and in another path, inverse delay was provided. Although the split pulses are sequentially overlapped in front of the PMT, any adverse effects of the time delay between the twice excitations were not detected in the dual-comb signals. The reduction of the Doppler-broadening background is apparent in the magnified view of the spectra (Fig. 4(b)). The background peak reduces with increasing the pulse delay. The ratios between the background peaks and Doppler-free spectral peaks are 6.9%, 1.9%, and 0.1%, corresponding to delays of 1 mm, 5 mm, and 10 mm. In the case of 10 mm delay, the reduction of the Doppler-broadening background is sufficient, and is extremely useful for precise spectroscopy.

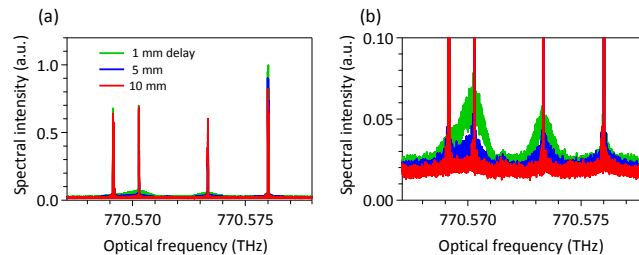


Fig. 4. (a) Doppler-free spectra of the $5S_{1/2} - 5D_{5/2}$ transition measured with split pulse delays of 1 mm (green), 5 mm (blue), and 10 mm (red). (b) Magnified view around the Doppler-broadening background.

3.3 Reduction of noise floor using coherent averaging of the fluorescence signal

The coherent averaging technique has been widely used in dual-comb spectroscopy. However, in dual-comb fluorescence detection, it has not previously been applied. In dual-comb spectroscopy without coherent averaging, Fourier processing of every interferogram including huge number of data points corresponding to $M = f_{\text{rep}}/\Delta f_{\text{rep}}$ cannot keep up with the continuous data stream; thus, averaging times and attainable SNR is limited by the digitizer memory. Coherent averaging is a method to average the time domain dual-comb signals [23,24]. The method enables a long period of continuous real-time averaging, and thus removes the limitation of digitizer memory and realizes high-SNR measurements. In addition, time-domain averaging can suppress detector noise and shot noise which obscure weak dual-comb beats. Therefore, a dramatic sensitivity improvement is expected especially in the dual-comb fluorescence detection by using coherent averaging.

Coherent averaging is only successful during the mutual coherence time of two combs. Our dual-comb source has enough coherence time as shown in our previous study, with the relative linewidth at 1550 nm being 2.6 mHz [7]. Fluorescence dual-comb beat spectra have been reported in previous works [11,12], then, we check the linewidth of dual-comb beats in fluorescence signal. Figure 5(a) shows Doppler-limited two-photon absorption dual-comb spectrum of the $5S_{1/2} - 5D_{5/2}$ transition measured by an RF spectrum analyzer. The fluorescence RF beat with an interval of $\Delta f_{\text{rep}} = 50$ Hz was fully resolved, and the linewidth of a beat was approximately 1.1 Hz as shown in Fig. 5(b). The line width was limited by a resolution of the RF spectrum analyzer. In the fluorescence dual-comb spectroscopy, the beats are created by modulation of the excited state population, and these are essentially different from heterodyne beats between comb modes. Even though fluorescence is incoherent emission, the narrow relative linewidth of the dual-comb source was transferred to amplitude modulation linewidth of the fluorescence signal. Therefore, the coherent averaging scheme was applicable to the fluorescence detection based dual-comb spectroscopy.

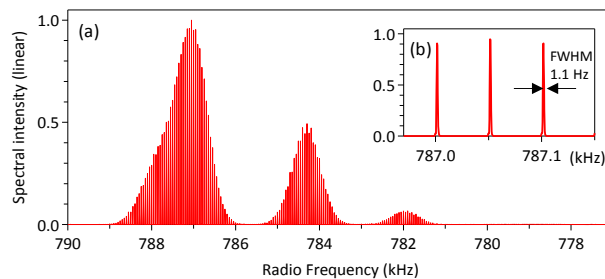


Fig. 5. (a) RF spectrum of fluorescence signal measured by an RF spectrum analyzer resulting in the mode-resolved Doppler-limited $5S_{1/2} - 5D_{5/2}$ spectrum. (b) Magnified view of the spectrum. The mode intervals are corresponding to $\Delta f_{\text{rep}} = 50$ Hz, and the full-width half-maximum (FWHM) = 1.1 Hz.

To perform long term averaging of the signal beyond the coherence time, linear phase correction should be applied [24]. The phase drift information can be obtained from a portion of the interferogram around a center burst. In contrast, the resulting fluorescence signals have no center burst, and it is difficult to use the phase correction scheme. Thus, the fluorescence signal was coherently averaged for a short period below the coherence time, and Fourier transformed at the interval of the averaging period. The obtained spectra are continuously integrated, and we achieve persistent averaging of fluorescence spectra.

To demonstrate the ability of the coherent averaging technique improving the fluorescence detection sensitivity, we show two spectra obtained by using coherent averaging and by averaging of Fourier transformed spectra. To implement the coherent averaging, the relationships between the repetition frequencies and offset frequencies are fixed as $f_{\text{rep},1}/\Delta f_{\text{rep}} = M$ and $\Delta f_{\text{co},1}/\Delta f_{\text{rep}} = C$, respectively, where M and C are integers. Even

when $f_{\text{rep},1}$ is changed, M and C are held constant. In this experiments, Δf_{rep} was set to 100 Hz, thus the minimum period of the data acquisition was 10 ms. The two measurements were performed using identical conditions, with incident power of 10 mW, cell temperature of 40 °C, and an averaging time of 20 s for each scan point. For the first results shown in blue plots in Figs. 6, coherent averaging was not used. The single-shot fluorescence signal acquired in 10 ms (Fig. 6 (a)) was Fourier transformed and resulting spectra was integrated 2000 times. In addition, for the second results shown in red plots, the coherent average of 10 fluorescence signals (Fig. 6 (a)) over 100 ms was Fourier transformed and the resulting spectrum was integrated 200 times. In both of the measurements, we used a 1/10 frequency divider for the f_{rep} sampling clock to reduce data and memory burden that became a problem in the first measurement. The use of the divider also reduces the Nyquist frequency to $f_{\text{rep}}/20$, but the measurement range is enough for our targets and the resolution is not degraded. The averaged Doppler-free spectra of $5S_{1/2} - 5D_{3/2}$ and $5D_{5/2}$ transitions are shown in Figs. 6(b) and (c), respectively. Assignment of the lines, isotope, and total angular momentum F'' in the ground state, are displayed near the transitions. As shown in Fig. 6(b), although a transition line of the ^{87}Rb , $5S_{1/2}$ ($F'' = 1$) to the $5D_{3/2}$ state was buried under the noise floor in the first measurement, a peak of the line appeared in the second measurement. The noise floors of the spectra are significantly reduced thanks to the noise suppression employing the time-domain averaging of the fluorescence signals. The reduction of the noise floor reduces the minimum detection limit and improves sensitivity of the measurement. Spectral peaks are slightly reduced because of the additional phase and amplitude noises caused in EDFA, SHG, and free-space measurement path.

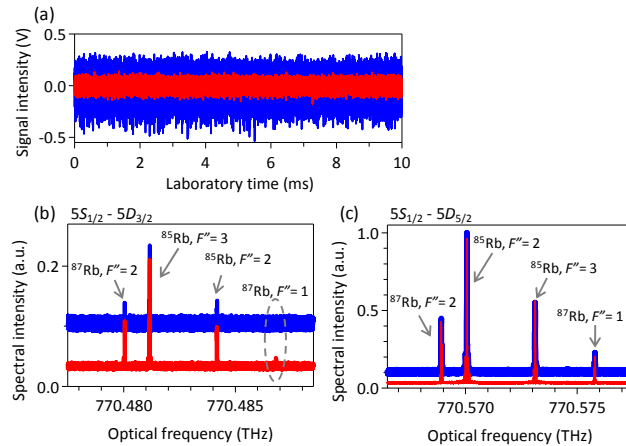


Fig. 6. (a) Single-shot of fluorescence signal (blue) and coherently averaged signal over 10 times (red). Obtained spectrum of (b) the $5S_{1/2} - 5D_{3/2}$ and (c) the $5S_{1/2} - 5D_{5/2}$ transition after same averaging time of 20 s and spectral interleaving. Noise floor of the spectrum resulting from the single-shot fluorescence signal (blue) was higher than the noise floor obtained from the coherently averaged signal (red)

3.4 Line profile and absolute frequency measurement of hyperfine spectra

We determined absolute transition frequencies of the hyperfine components of the $5S_{1/2} - 5D_{5/2}$ transition using the elimination of Doppler-broadening background and suppression of the noise by coherent averaging. The measurement parameters are as follows: incident power of 8 mW, cell temperature of 40 °C, spectral sampling step of 400 kHz (which corresponds to interleaving the f_{rep} with 140 points), and $\Delta f_{\text{rep}} = 100$ Hz. The coherently averaged fluorescence signal over 20 ms was Fourier transformed and integrated 200 times, thus the total acquisition time was 100 min. Figure 7 shows magnified views of components of the $5S_{1/2} - 5D_{5/2}$ transition and its assignments of total angular momentum F' of excited state. The observed spectral linewidths are 4–5 MHz, and most of the hyperfine splittings of the $5D_{5/2}$ state are fully resolved. The observed linewidths are

broadened relative to the natural width of the transition, ~ 660 kHz. The broadenings are mainly caused by residual Doppler-broadening. In the two photon spectrum obtained by counter-propagating photons with different frequencies, the residual Doppler-broadening appears as $f(v_z) \times (f_n - f_m)/c$, where $f(v_z)$ is a velocity distribution of the atoms and c is the velocity of light. Therefore, the residual Doppler-broadenings depend on variety of mode pairs and thus spectral profiles of combs. The spectral width of our dual-comb source was 5 nm, and a similar sub-Doppler linewidth was reported in a study of single-comb spectroscopy with the same spectral width [21]. The obtained hyperfine spectra are fitted by Voigt functions (blue curves) which are convolutions of Gaussian and Lorentzian functions. We simply assumed that the Lorentzian represents homogeneous broadenings that indicate natural width and transit-time broadening, and the Gaussian represents inhomogeneous broadenings that indicate residual Doppler-broadening and contributions of comb mode linewidths. We can use a flat baseline function in the fitting thanks to the elimination of Doppler-broadening background. Fitting residuals are shown above the spectra. The residuals of some transitions that have no overlap with neighboring transitions exhibit symmetric but systematic features. The residuals indicate the contributions from the other effect, such as intensity distributions depending on the frequency difference of mode pairs, and strong stepwise excitation introduced by a portion of the comb spectra.

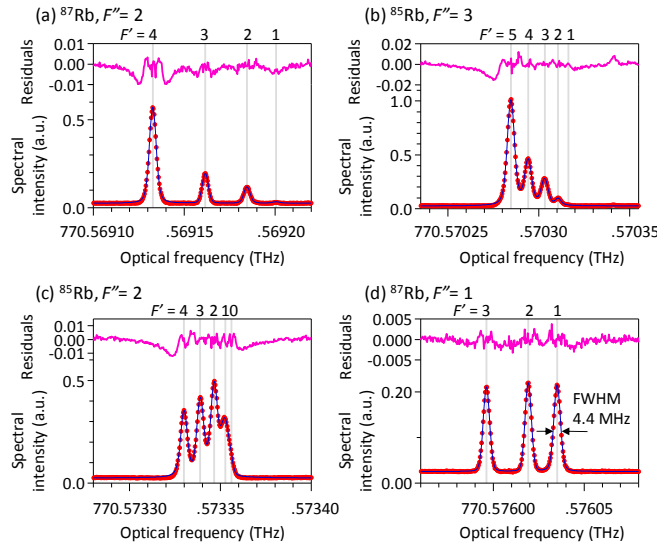


Fig. 7. Doppler-free two-photon absorption spectra, fitted Voigt functions and residuals of hyperfine components of $5S_{1/2} - 5D_{5/2}$ transition. Assignments of the transitions are shown above the graph, (a) $5S_{1/2}$ (^{87}Rb , $F'' = 2$) - $5D_{5/2}$, (b), $5S_{1/2}$ (^{85}Rb , $F'' = 3$) - $5D_{5/2}$, (c), $5S_{1/2}$ (^{85}Rb , $F'' = 2$) - $5D_{5/2}$, (d) $5S_{1/2}$ (^{87}Rb , $F'' = 1$) - $5D_{5/2}$.

Absolute frequencies of the line centers of fitted Voigt functions are listed in Table 1. The previously reported values from the Comité International des Poids et Mesures (CIPM) [28] are fourth column and the values in parentheses represent the uncertainty of reported values. Here, we consider the uncertainty of our measurement. Stabilized comb mode uncertainties are determined by the uncertainty of the referenced GPS disciplined clock, which is about 2.3 kHz in this transition frequency. Fitting deviations of center frequency are larger than the comb mode uncertainty. The deviations are a few kHz to several tens of kHz. The residuals of the fittings are symmetric respect to each sub-Doppler line, but it is ranging larger than the full width at half maximum of a line. The residuals influence the determination of center frequencies of the neighboring lines each other. Here an effect of light shift is also a part of systematic uncertainty. However, the effect is sufficiently smaller than the fitting deviations. Therefore, the uncertainty of our

measurement are mainly caused by disagreement with the Voigt function and observed spectral line shapes.

The fifth column in Table 1 shows differences between CIPM values and obtained values in this work. Due to the large overlap and small spectral intensity, the center frequencies of the ^{85}Rb , 3 – 1 and 2 – 0 lines are fixed to values in the reference when the fitting was performed. The other lines of ^{85}Rb also have large overlaps with neighboring lines, then some lines show relatively large discrepancies. On the other hand, differences of ^{87}Rb lines are less than 100 kHz because hyperfine splittings are larger than that of ^{85}Rb , thus the effect of the neighboring lines are smaller. Finally, as shown in the results, the spectral lines with small effect of fitting residuals of neighboring lines show good agreement with the values in the CIPM report.

Table 1. Absolute frequencies of hyperfine components of $5S_{1/2} - 5D_{5/2}$ transition

Ground state	F'	This work (kHz)	CIPM (kHz)	Difference (kHz)
$^{87}\text{Rb } F''=2$	4	770 569 132 733	770 569 132 748 (18)	-15
	3	770 569 161 613	770 569 161 572 (18)	41
	2	770 569 184 579	770 569 184 526 (18)	53
	1	770 569 200 542	770 569 200 466 (18)	76
$^{85}\text{Rb } F''=3$	5	770 570 284 633	770 570 284 750 (10)	-117
	4	770 570 294 147	770 570 294 186 (18)	-39
	3	770 570 303 257	770 570 303 206 (18)	51
	2	770 570 310 607	770 570 310 812 (18)	-205
	1	-----	770 570 316 292 (28)	----
$^{85}\text{Rb } F''=2$	4	770 573 329 855	770 573 329 940 (18)	-85
	3	770 573 338 880	770 573 338 938 (18)	-58
	2	770 573 346 520	770 573 346 524 (18)	-4
	1	770 573 352 617	770 573 352 012 (22)	605
	0	-----	770 573 354 918 (52)	----
$^{87}\text{Rb } F''=1$	3	770 575 996 200	770 575 996 260 (18)	-60
	2	770 576 019 192	770 576 019 216 (18)	-24
	1	770 576 035 113	770 576 035 150 (18)	-37

4. Conclusion

We have demonstrated Doppler-free two-photon absorption spectroscopy of $^{87,85}\text{Rb}$ using dual-comb spectroscopy based on fluorescence detection for precise and highly sensitive measurement. We measured the $5S_{1/2} - 5D_{5/2}$ and $5D_{3/2}$ transitions simultaneously, and obtained the Doppler-broadened and Doppler-free spectra corresponding to the excitation with co-propagating and counter-propagating photons, respectively.

To realize precise spectral measurement, we employed a pulse shaping scheme in the dual-comb spectroscopy for the first time. The resulting Doppler-free two-photon spectra have almost completely flat background. The ratio of the Doppler-free and Doppler-background peaks is 0.1%. In our case, the effect of the Doppler background to the fitting error is expected to be small, but the background reduction technique is useful to realize higher precision of two-photon dual-comb spectroscopy. In addition, we investigated the coherence of dual-comb beats in the fluorescence signal. We confirmed that the coherence of the two combs are transferred to dual-comb beats in the fluorescence signal by measuring the linewidth of the fluorescence RF spectra. The observed linewidth was limited by the resolution of the RF spectrum analyzer, and was 1.1 Hz. We applied the coherent averaging scheme to the fluorescence based dual-comb spectroscopy, and

demonstrated the great sensitivity improvement. The observed hyperfine resolved spectra with linewidths of 4–5 MHz are successfully fitted to the Voigt functions, but the systematic residuals indicated the contribution of excitation processes with broadband frequency combs. The precision of the absolute frequency is better than 100 kHz for the hyperfine components of ^{87}Rb which do not have overlaps of the lines.

The Doppler-free two-photon dual-comb spectroscopy is a widely applicable high-resolution and broadband spectroscopic technique. Moreover, the employment of coherent averaging improves the sensitivity, and expands the applicable targets. The pulse-shaping scheme enables obtaining a flat baseline spectrum and reveals accurate line shapes of the Doppler-free spectra. However, to realize further improvement of the precision, line shape studies of the spectra excited by broadband pulses are important to get a best fitting function.

Funding

Japan Science and Technology Agency (JST) ERATO MINOSHIMA Intelligent Optical Synthesizer (IOS) Project (JPMJER1304); JSPS KAKENHI grants (16J02345, 17K14435).

Acknowledgments

We thank Eiji Tokunaga, Kazuaki Nakata, Naoyuki Shiokawa, and Masayuki Sirakawa (Tokyo University of Science) as well as Akifumi Asahara and Ken'ichi Kondo (UEC) for their assistance in the early stages of developing the Er-doped fiber lasers. We also thank Atsushi Onae, Hajime Inaba, and Sho Okubo (AIST) for their valuable advice concerning the dual-comb system setup, and Masaaki Hirano, Yoshinori Yamamoto, and Takemi Hasegawa of Sumitomo Electronics Inc. for providing us with highly nonlinear fibers.